

Unoccupied band structure of wurtzite GaN(0001)

T. Valla and P. D. Johnson

Department of Physics, Brookhaven National Laboratory, Upton, New York 11973

S. S. Dhesi and K. E. Smith

Department of Physics, Boston University, Boston, Massachusetts 02215

D. Doppalapudi and T. D. Moustakas

Department of Electrical and Computer Engineering, Boston University, Boston, Massachusetts 02215

E. L. Shirley

NIST, PHY B208, Gaithersburg, Maryland 20899

(Received 29 July 1998)

We report an inverse photoemission study of the unoccupied states of thin-film *n*-type wurtzite GaN. For incident electron energies below 30 eV, free-electron bands do not provide a good description of the initial state. However, using a calculated quasiparticle band structure for the initial state, we can obtain good agreement between our measurements and the calculated low-lying conduction bands. No evidence of unoccupied surface states is observed in the probed part of the Brillouin zone, confirming earlier angle resolved photoemission studies, which identified the surface states on GaN(0001) as occupied dangling bond states, resonant with the valence band. [S0163-1829(99)09007-4]

I. INTRODUCTION

Wide-gap nitride semiconductors (such as GaN, InN, AlN, and their alloys) are an important class of electronic materials. Rapid progress is currently being made in the development of electronic devices based on heteroepitaxially grown wurtzite films of these nitrides.¹ Extensive investigations of the basic electronic structure of such films are in progress, and the results of soft x-ray emission (SXE), soft x-ray absorption (SXA), and angle-resolved photoemission (ARPES) studies of *n*-type thin-film wurtzite GaN have been reported recently.^{2,3} SXE and SXA measure the bulk valence and conduction-band partial density of states, while ARPES measures the dispersion of both surface and bulk valence-band states. Missing from these studies are measurements of the *dispersion* of the unoccupied conduction-band states. Because the unoccupied bands are the final electron states in any absorption event, a detailed measurement of their structure is of importance.

We report here the first measurement using inverse photoemission spectroscopy (IPES) of the band structure of the unoccupied states in *n*-type thin-film wurtzite GaN. IPES provides information for the unoccupied states equivalent to that provided by ARPES for the occupied states. We find that, for incident electron energies below 30 eV, free-electron bands do not provide a good description of the initial IPES states. However, guided by a calculated quasiparticle band structure for the initial IPES state, we obtain good agreement with the calculated low-lying quasiparticle conduction bands.⁴ Combining the present momentum-resolved IPES studies with the earlier ARPES results,² we are able to confirm the direct gap of 3.5 eV predicted in quasiparticle band-structure calculations.⁴

II. EXPERIMENTAL AND NUMERICAL DETAILS

The IPES measurements were made using an off-Rowland circle high-resolution grating spectrometer that has been discussed in detail elsewhere.⁵ This spectrometer allows the detection of photons in the range of 9 to 35 eV. By varying the energy of the incident electrons one can measure the photon-energy dependence of the favored transitions into different final states close to the Fermi level. The overall energy resolution of the instrument was approximately 0.3 eV.

The wurtzite GaN films studied were grown using electron cyclotron resonance assisted molecular-beam epitaxy on sapphire substrates as described elsewhere⁶ and were Si doped *n* type with carrier concentrations of $5 \times 10^{17} \text{ cm}^{-3}$. The films were of high quality as determined from resistivity, mobility, carrier concentration, and photoluminescence measurements. Samples were transported in air, rinsed in a 1:10 solution of concentrated HCl and deionized water, mounted in the analyzer chamber (base pressure $< 3 \times 10^{-10}$ mbar), and outgassed for several hours at 900 °C. The sample surfaces were cleaned using a procedure similar to that of Bermudez *et al.*:^{7,8} first a Ga layer was evaporated onto the surface, but was then partially removed by repeated annealing to 900 °C, resulting in the simultaneous removal of much of the surface oxygen. The sample was next subjected to repeated cycles of sputtering with 1.5 keV N_2^+ ions and annealing in ultra-high vacuum at 900 °C. Auger electron spectroscopy indicated that this procedure reduced the surface oxygen concentration levels to less than 2%, with no indication of any other surface contamination. The sample exhibited a sharp (1×1) low-energy electron diffraction pattern on a low background with no evidence of a surface reconstruction or faceting. All measurements re-

ported here were performed with the sample held at room temperature. Binding energies are referenced to the E_F , determined from an atomically clean piece of Ta foil in electrical contact with the sample.

Spectra were interpreted by considering the unoccupied states between Γ and A along the Δ line. Wave functions for electron states in the bulk were computed using the local-density approximation^{9,10} for exchange and correlation within the pseudopotential/plane-wave framework.¹¹ Wave functions were constructed from a smaller basis set of linear combinations of plane waves (“optimal” basis functions), which are described in Ref. 12. For w -GaN, the optimal basis set was constructed to optimally span electron states at Γ and both A 's (i.e., on both hexagonal faces of the Brillouin zone). States in the eight occupied valence 32 lowest unoccupied bands were considered, an 81-Ry plane-wave cut off was used to describe electron states, whereas B functions¹² were computed with a 100-Ry cutoff. 110 B functions were used. For further details of aspects of the calculation of electron wave functions, the reader is referred to Ref. 12. Band (quasiparticle) energies were taken as the energies obtained in the local-density approximation but corrected to include self-energy (many-body) corrections. Corrections to the band gap are taken from Rubio *et al.*⁴ Besides a correction to the local-density approximation band gap, the results of Ref. 4 also suggest a substantial stretching of the energy scale for unoccupied bands, so that self-energy corrections become increasingly positive for higher and higher conduction bands. Such a trend was doubted by Lambrecht *et al.*¹³ and no stretching was assumed in this work. Therefore, the assumed quasiparticle energies reflect the local-density approximation energies plus a constant offset to achieve a band gap of 3.5 eV.

To compute angle-resolved inverse photoemission spectra, one requires initial- and final-state electron wave functions and energies, as well as $\mathbf{p} \cdot \mathbf{A}$ matrix elements connecting initial and final states. A complete treatment would necessitate some description of electron wave functions near the surface of a semi-infinite solid. An incident electron with some energy E should have a plane-wave-like wave function in the vacuum, but the wave function should have a spatial character similar to that of isoenergetic conduction-band states in the solid. The transition matrix element between an incident initial state and band final states may be written as

$$\langle \Phi_{n\mathbf{q}} | \mathbf{p} \cdot \mathbf{A} G_{\mathbf{q}}(E) | \Psi_{\text{inc}} \rangle \propto \sum_{n'=\text{empty}} \langle \Phi_{n\mathbf{q}} | \mathbf{p} \cdot \mathbf{A} | \Phi_{n'\mathbf{q}} \rangle \times \langle \Phi_{n'\mathbf{q}} | \Psi_{\text{inc}} \rangle (E + i\Gamma - \varepsilon_{n'\mathbf{q}})^{-1}.$$

Here, $|\Phi_{n\mathbf{q}}\rangle$ is a bulk state in band n with crystal momentum \mathbf{q} , having quasiparticle energy $\varepsilon_{n\mathbf{q}}$. Γ accounts for quasiparticle life-time broadening (or, alternatively, the finite electron mean-free path at energy E). The above expression relies on decomposition of an incident electron wave function into bulk conduction bands in the solid. Smallness of photon momentum permits consideration of vertical transitions only. Such an expression may be deduced from the matrix element relevant in the (time-reversed) direct photoemission case.

At sufficiently high kinetic energies, the incident electron state could be approximately represented as a plane wave without severe approximation. However, the low kinetic energies characterized by this work suggest that an equally adequate treatment of the incident electron state in this case would be rather involved. Decomposition of this state into bulk-like states in the solid is complicated both by the strong effects of the crystalline potential at such low energies and by uncertainty as to how to match the incident vacuum plane-wave with bulk-like states at the surface. Instead, we have noted that free-electron plane-wave states within momentum $\mathbf{G} + \mathbf{q}$ [$\mathbf{G} \equiv (002), (003)$] are the plane-wave states closest in energy to the initial state. By symmetry, only a subset of the real band states along the Δ line should couple at all to a normally incident plane wave, and those that do couple have nonzero $(00N)$ Fourier components of $u_{n\mathbf{q}}(\mathbf{r}) = \Phi_{n\mathbf{q}}(\mathbf{r})/\exp[i\mathbf{q} \cdot \mathbf{r}]$ for either odd N or even N , but not both. As a crude approximation, therefore, the photon emission spectrum (as a function E and photon energy $h\nu$) may be characterized by

$$S(h\nu, E) \propto \sum_{n=\text{empty}} \sum_{\mathbf{q}} \sum_{\mathbf{e}} \{ |\langle \Phi_{n\mathbf{q}} | \mathbf{p} \cdot \mathbf{e} G_{\mathbf{q}}(E) | 002 \rangle|^2 + |\langle \Phi_{n\mathbf{q}} | \mathbf{p} \cdot \mathbf{e} G_{\mathbf{q}}(E) | 003 \rangle|^2 \} \delta(h\nu + \varepsilon_{n\mathbf{q}} - E),$$

where \mathbf{e} denotes the electric-field polarization vector. This is the expression that was used. This approximates the sizes of matrix elements, yet all energy-conservation and symmetry considerations are taken into account. Therefore, meaningful comparison between theoretical and measured spectral features can be done. We have used $\Gamma = 1$ eV (2 eV full width at half maximum), and Gaussian energy broadening of the δ function was used to effect 0.5 eV resolution.

III. RESULTS AND DISCUSSION

Figure 1 shows inverse photoemission spectra recorded with the electron beam incident along the normal of the GaN(0001) surface, with initial energies in the range from 12.3 to 29.8 eV above E_F . For the wurtzite (0001) surface, normal-incidence IPES probes the states with momenta along the $\Gamma\Delta A$ symmetry line in the bulk Brillouin zone. The spectra clearly show dispersive features that extend from ~ 2 up to 11 eV above E_F . These features correspond to photon emission resulting from radiative transitions into low-lying final states in the inverse photoemission process. Under the assumption that transitions from the initial states to these final states are direct (i.e., energy and momentum conserving), it is possible to reconstruct the dispersion of the final, as well as of the initial IPES states. It is important to keep in mind that in each spectrum in Fig. 1, the observed final states have approximately the same wave vector (because each spectrum involves a particular range of initial states). This is the primary difference between IPES as performed here, and isochromat IPES or ARPES spectra, and it allows us to conduct a simultaneous mapping of both initial and final bands.

As is the case when extracting band dispersion for occupied states using ARPES, the normal component of the wave vector of the unoccupied states (k_{\perp}) cannot be determined absolutely by the IPES experiment. The lower bands (final state in IPES, and initial in PES) are commonly mapped

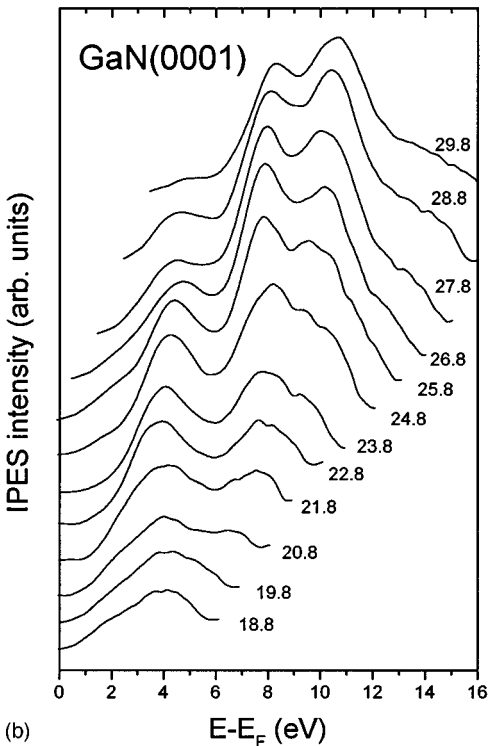
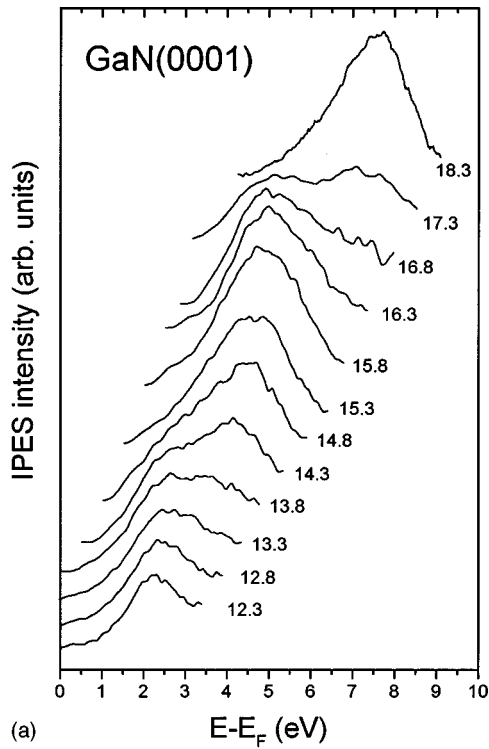


FIG. 1. IPE spectra of GaN(0001) surface recorded at normal incidence for the incident electron energy in the range from 12.3 to 18.3 eV (a), and from 18.8 to 29.8 eV (b). Energies are referenced to the Fermi level.

using empirical free-electron-like upper bands (initial state in IPES, and final in PES), but for many materials this approximation is found to be incorrect.

From Fig. 1, it is clear that the dispersive features approach extremal energies at certain values of the initial energy. These extrema can be used to identify the position in k

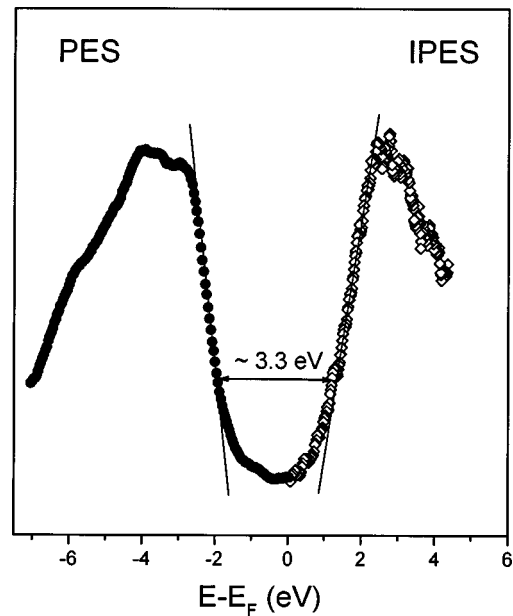


FIG. 2. IPE spectrum recorded at the Γ point (13.8 eV spectrum from Fig. 1) (right), and PES spectrum (left) taken at the same point (Ref. 2). The obtained value of momentum-resolved gap at this point is ≈ 3.3 eV.

space of high-symmetry points within the zone. In our case these points correspond to the zone center (Γ) or to the zone boundary (A). The first of such extrema is observed at 1.5–2 eV above the Fermi level E_F for the initial energy of 13.8 eV [Fig 1(a)]. This is the lowest state seen in the whole series of spectra, and we assign it to the bottom of the conduction band at the zone center Γ_1 . It disperses upwards, and acquires a maximal energy of 4.5–5 eV above E_F (at an initial state energy of 16–17 eV) where it becomes degenerate with a less dispersive state. We assign this point to the zone boundary and thus designate the observed maximum as the $A_{1,3}$ point. The same dispersion (from Γ to A) is repeated in Fig. 1(b) between 18.8 eV (Γ) and 25–27 eV (A) initial electron energy. In addition, transitions to two other bands can be seen in Fig. 1(b) at higher initial energies. One of these features has minimal energy (~ 7 eV) at the same initial state energy (25–27 eV) where the two lower bands acquire their maxima. Further evidence for the proper assignment of the zone boundary (A) is that, whenever k_{\perp} passes through it (16–17 eV or 25–27 eV initial state energies), an intensity transfer from the lower final states to the higher ones occurs with increasing initial state energy. The same effect is observed for metal surfaces and can be understood in terms of a simple, two-band nearly free-electron model of the (inverse) photoemission process close to the zone boundary.¹⁴

We can combine our IPES Γ point emission spectrum for the conduction-band states with a previously published ARPES Γ point emission spectrum for the valence band to determine the direct gap. The momentum-resolved gap of ≈ 3.3 eV shown in Fig. 2, is in good agreement with the calculated gap of 3.5 eV in quasiparticle band-structure calculations. The latter comparison is appropriate in that the quasiparticle band gap represents the difference between the ionization potential and the affinity level. Figure 2 is also direct evidence of the band bending near the (0001) surface,

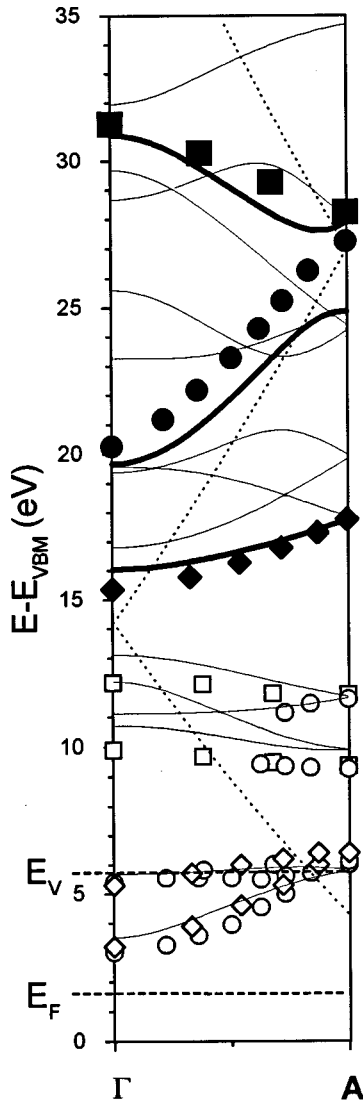


FIG. 3. Comparison of measured band structure (symbols) and quasiparticle band-structure calculation (solid lines). Thick lines denote bands which couple strongly to $G=(002)$ plane wave. Solid symbols represent experimental points of initial IPES states, while open symbols denote corresponding final states. An error is roughly represented by the size of the symbol. The free-electron parabola used as the final PES state in Ref. 2 is shown for comparison (dotted line). Energies are referenced to the valence-band maximum (VBM).

which for our sample is measured to be ≈ 1.5 eV. This observation allows us to reference measured energies to the VBM.

In Fig. 3 we compare the experimentally determined dispersion of the unoccupied bands with the calculated quasiparticle band structure. The energy scale is referred to the valence-band maximum (VBM). The position of the vacuum level indicates the measured value of the work function (4.30 ± 0.15 eV, as measured by the retarding field method). The experimental points in the band dispersions are determined by first identifying the critical points and then allowing the experimental dispersion to take the same form as the calculated dispersion for the final states. In fact, this approach of determining k_{\perp} by comparison with calculated final state bands is similar to that used in an earlier PES study

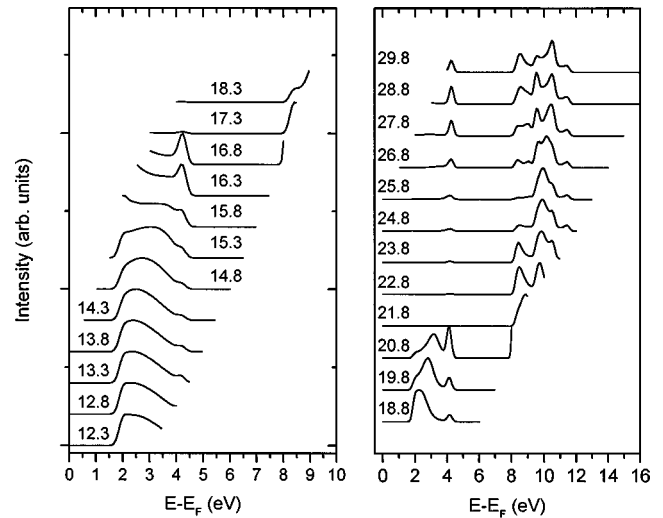


FIG. 4. Theoretical inverse photoemission spectra as described in the text. Intensity is shown as a function of electron final state energy, for several values of incident electron energy, indicated by each spectrum (measured in eV).

of III-V compound semiconductors.¹⁵ It is clear from the figure that reasonable agreement between experiment and calculation is obtained for all bands that have the appropriate symmetry for observation. The initial state bands at higher energies are constructed by adding the appropriate photon energy to the final state bands.

The most sensitive point in determining the band structure from IPES spectra is proper identification of the critical points. The critical points determined experimentally from the spectra in Fig. 1 do not agree with those expected if the initial IPES states were free-electron like. For example, instead of only one band crossing from Γ to A as expected from a free electron parabola, we observe two crossings in our range of initial energy. Clearly, the free-electron approximation for the upper IPES bands in GaN is not valid. Note, however, that a free electron final state was used to extract the valence-band dispersion in the recent ARPES study² and gave good agreement with the quasiparticle band structure.⁴ This is due to the fact that higher photon energies of 35 to 100 eV were used in the ARPES study (and consequently, higher final state bands were probed), while much lower energy bands are being probed here. The higher in energy, the more free electron like the empty states should become. A low photon energy ARPES study might have to use the empty states determined here for the final states in extracting the valence-band structure.

In Fig. 4 we show calculated IPES spectra as a function of incident electron beam energy. A detailed examination of these calculated spectra shows moderate agreement with the experimental spectra presented in Fig. 1. In particular, at low-incident energies, a feature is observed close to the bottom of the conduction band. As the incident energy is increased, this feature disperses to higher energies in the conduction band. At the higher energies corresponding to the spectra in Fig. 1(b), the calculation reproduces much of the behavior experimentally observed for the features in the range 2–4 eV above the Fermi level and in the range 8–12 eV above E_F . The simulated spectra suggest that further

attention to describing the electron initial state wave function may benefit future work.

Our calculation indicates that the direct transitions resulting in these spectra correspond to initial states that weight the (002) plane wave. These bands are highlighted in Fig. 3 with the solid lines. As can be seen from the figure, these latter lines closely parallel the experimentally determined initial states and strengthen our assignment of critical points.

IV. CONCLUSIONS

Our IPES study has allowed the first detailed study of the dispersion of the conduction bands in wurtzite GaN. In addition, the nature of the present experiment allows simultaneous determination of several of the higher lying conduction bands. Good agreement is found between the experimentally measured conduction bands and the same bands determined in a quasiparticle band calculation, provided that the energy scale for the conduction-band complex is assumed to be like the energy scale of the local-density approximation results. That is, the conduction band is found

to lie where predicted in the quasiparticle calculations, except that intervals between lower and higher conduction bands are similar to those found in the local-density approximation, and not as large as found by Rubio *et al.*⁴

By combining the present measurements with an earlier PES study, we find the momentum-resolved band gap at the center of the zone to be ≈ 3.3 eV, confirming the direct gap of 3.5 eV predicted in calculations. Finally, we note that no unoccupied surface states have been identified in this study, an observation that confirms earlier ARPES studies that indicated the surface states on GaN(0001) represent occupied dangling bond states.²

ACKNOWLEDGMENTS

This work was supported in part by the Department of Energy under Contract No. DE-AC02-98CH10886 (P.D.I.) and the National Science Foundation under Grant No. DMR-9504948 (K.E.S.). T.D.M. acknowledges the support of the DoD/ARPA under Grant No. MDA972-96-3-0014.

¹*III-V Nitrides*, edited by F. A. Ponce, T. D. Moustakas, I. Akasaki, and B. A. Monemar, MRS Symposia Proceedings No. 449 (Materials Research Society, Pittsburgh, 1997).

²S. S. Dhesi, C. B. Stagarescu, K. E. Smith, D. Doppalapudi, R. Singh, and T. D. Moustakas, Phys. Rev. B **56**, 10 271 (1997).

³C. B. Stagarescu, L.-C. Duda, K. E. Smith, J. H. Guo, J. Nordgren, R. Singh, and T. D. Moustakas, Phys. Rev. B **54**, 17 335 (1996).

⁴A. Rubio, J. L. Corkhill, M. L. Cohen, E. L. Shirley, and S. G. Louie, Phys. Rev. B **48**, 11 810 (1993).

⁵P. D. Johnson, S. L. Hulbert, R. F. Garrett, and M. R. Howells, Rev. Sci. Instrum. **57**, 1324 (1986).

⁶T. Lei, M. Fanciulli, R. J. Molnar, T. D. Moustakas, R. J. Graham, and J. Scanlon, Appl. Phys. Lett. **59**, 944 (1991).

⁷V. M. Bermudez, Appl. Surf. Sci. (to be published).

⁸V. M. Bermudez, R. Kaplan, M. A. Khan, and J. N. Kuznia, Phys. Rev. B **48**, 2436 (1993).

⁹P. Hohenberg and W. Kohn, Phys. Rev. **136**, 864 (1964).

¹⁰W. Kohn and L. J. Sham, Phys. Rev. **140**, 1133 (1965).

¹¹For a review of this method, see W. E. Pickett, Comput. Phys. Rep. **9**, 115 (1989).

¹²E. L. Shirley, Phys. Rev. B **54**, 16 464 (1996).

¹³W. R. L. Lambrecht, S. N. Rashkeev, B. Segall, K. Lawniczak-Jablonska, T. Suski, E. M. Gullikson, J. H. Underwood, R. C. C. Perera, J. C. Rife, I. Grzegory, S. Porowski, and D. K. Wickenden, Phys. Rev. B **55**, 2612 (1997).

¹⁴S. D. Kevan, N. G. Stoffel, and N. V. Smith, Phys. Rev. B **31**, 1788 (1985).

¹⁵G. P. Williams, F. Cerrina, G. J. Lapeyre, J. R. Anderson, R. J. Smith, and J. Hermanson, Phys. Rev. B **34**, 5548 (1986).